Electronic Supplementary Material (ESI) for Journal of Materials Chemistry A.

Supporting Information

Pushing the Theoretical Capacity Limits of Iron Oxide Anodes: Capacity Rise of γ-Fe_2O_3 Nanoparticles in Lithium-ion Batteries

*Jialiang Tang, Claudia Edith Zavala Lugo, Salvador Francisco Acuña Guzmán, Geoffrey Daniel, Vadim G. Kessler, Gulaim A. Seisenbaeva, Vilas G. Pol**

Iron K edge X-ray absorption spectra were recorded at the wiggler beam line I811, MAX IV Laboratory, Lund, Sweden. The station was equipped with a Si (111) double crystal monochromator. XANES data collection was performed in fluorescence mode using a Stern–Heald–Lytle type detector equipped with a Canberra Industries Inc. PIPS photo diode. The primary beam flux, in a beam-spot size of 1 - 2 mm^2, was approximately 1011 photons per seconds. Higher-order harmonics were reduced by detuning the second monochromator crystal to 30% of maximum intensity. The energy scale of the X-ray absorption spectra were calibrated by assigning the first inflection point of the K edge of an iron foil to 7712 eV. The IFEFFIT program package (The IFEFFIT Reference Guide, Version 1.2) was used for the data treatment.

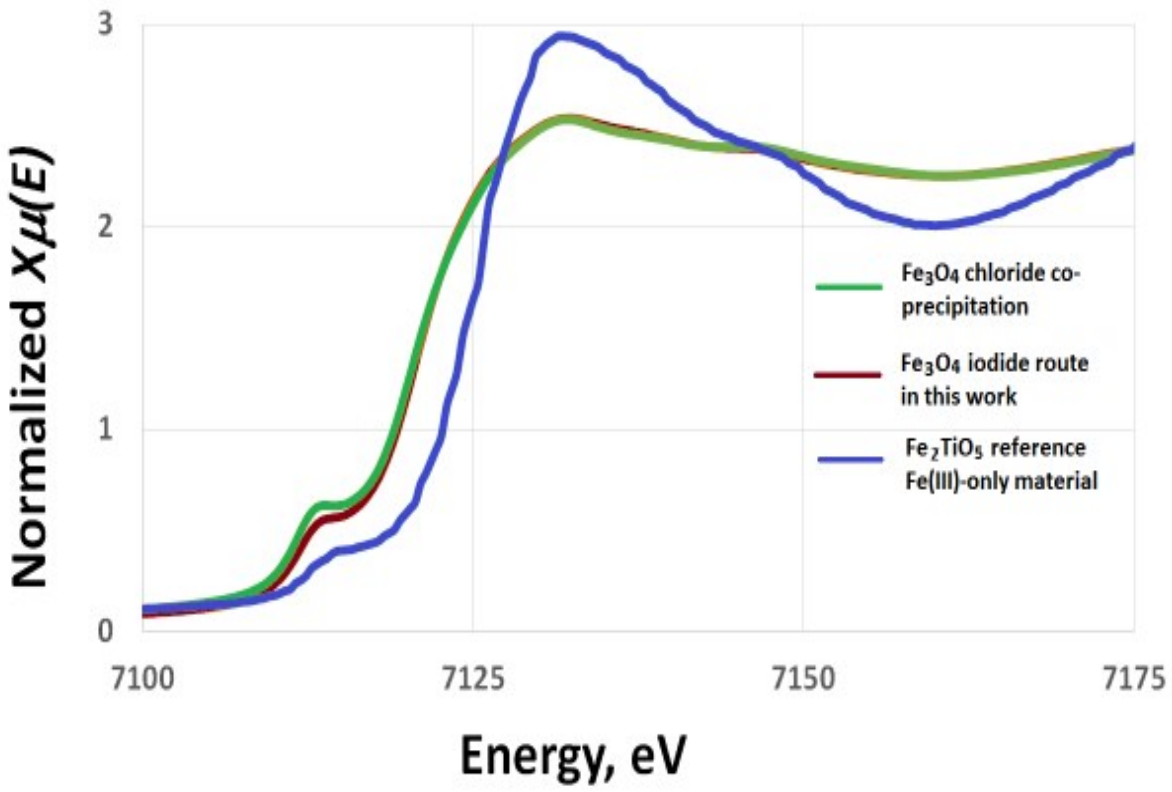

Fig. S1 XANES result of iron oxide nanoparticles before 3hr oxidation at 150°C.

Rate study of pure Super P carbon black electrode (80% Super P, 15% CMC, and 5% SBR) using 1M $LiPF_6$ with 3% FEC is summarized in Figure_S2a. As shown below, Super P carbon yields high capacity of ~250 mAh g^{-1} at 100 mA g^{-1} of Super P carbon and ~170 mAh g^{-1} at 1000 mA g^{-1} of Super P carbon; overall, the cell exhibits excellent rate capabilities. Therefore, it is important to account for the capacity contribution from Super P carbon in order to uncover the true electrochemical performance of synthesized iron oxide nanoparticles. Using the results from the rate study, specific capacity of Super P is plotted as a function of real run time (either the charge or discharge time of each cycle). A fitted line is also obtained to accurately estimate specific capacity of Super P carbon ($Q_{SupP} = Q_{fit}$) at any given run time (with goodness of fit $R^2 = 0.9519$).

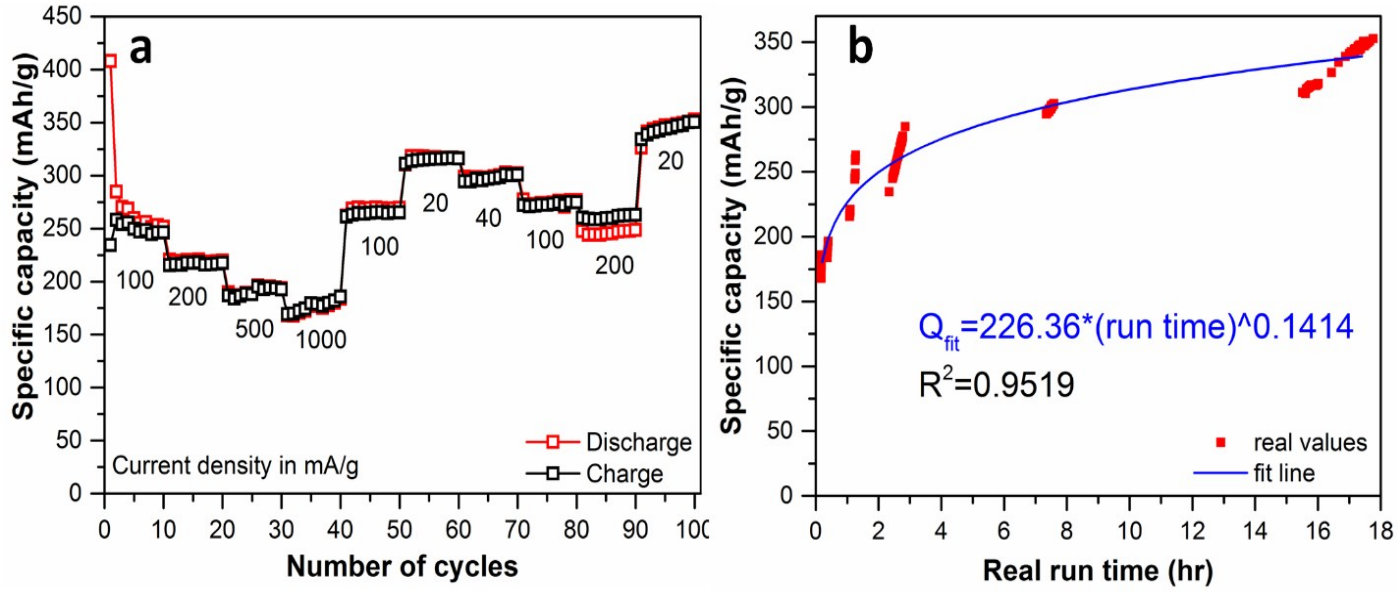

Fig. S2 Electrochemistry study of pure Super P carbon black electrode from 1 mV to 3V. a) Rate study, and b) specific capacity of Super P as a function of real run time.

Ex situ XRD spectra of pristine and cycled electrodes were collected to detect the changes in crystallinity of active material. For the cycled electrode, the cell was first charged to 3V to remove lithium from the active material; the electrode was then washed with dimethyl carbonate (DMC) to remove residual electrolyte and then dried under vacuum. Both electrodes were then covered with Kevlar tape on glass slides inside glovebox prior to XRD measurement. As shown below, after prolonged cycling, the crystallinity of iron oxide is lost and corresponding XRD peaks cannot be observed in the cycled electrode.

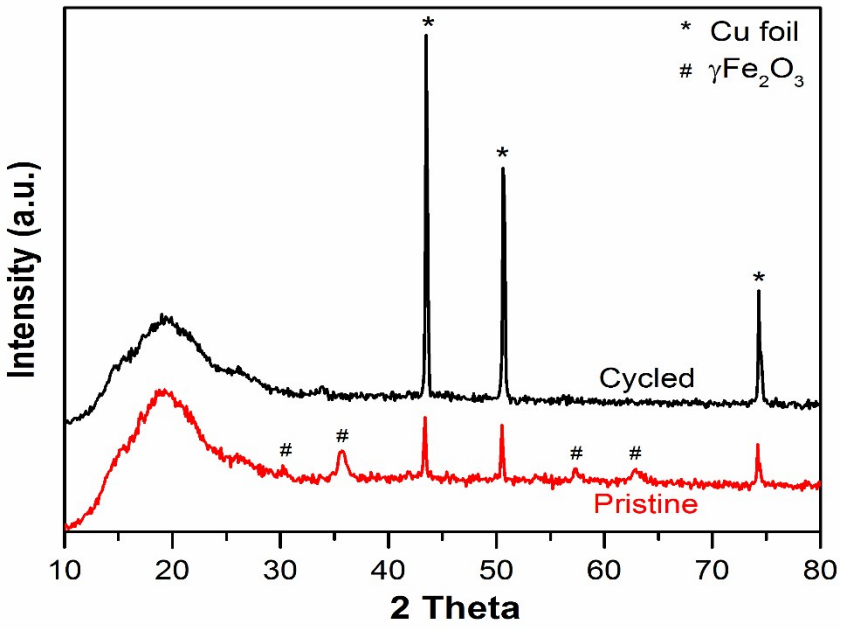

Fig. S3 Effect of cycling on the crystallinity of γ-Fe_2O_3. XRD plots of pristine and cycled electrodes.

To explore the origin of the peak development at discharge voltage of ~0.1V, pure Super P carbon electrodes were cycled in half cell configuration with and without 3% FEC additive in the electrolyte. Their dQ/dv plots are shown in the graph below. It can be seen that while these two cells exhibit resembling dQ/dV features as expected, the development of 0.1V peaks is only observable when 3% FEC is utilized.

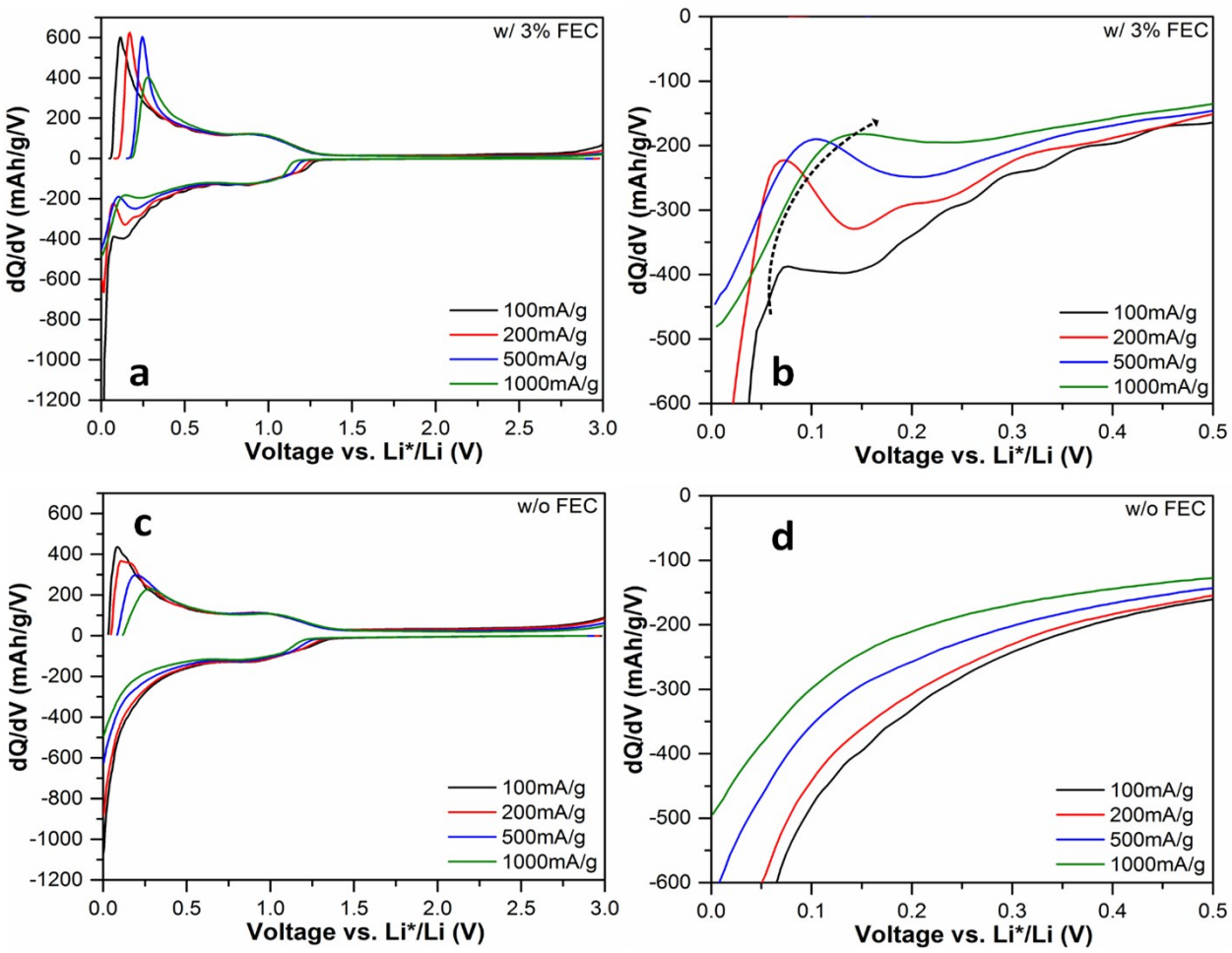

Fig. S4 Effect of FEC additive on cycling behaviors of Super P carbon black electrodes. dQ/dV plots of pure Super P half cells with a&b) 3% FEC, and c&d) no FEC additive.

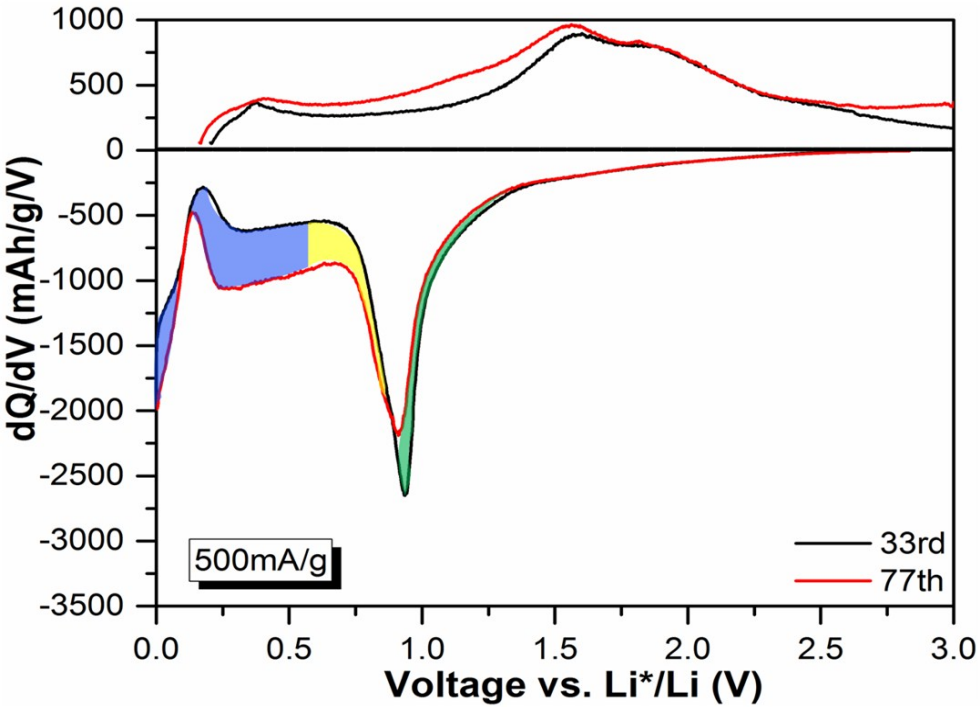

Fig. S5 dQ/dv plots of selected cycles at 500mA g^{-1} rates. Colored areas represent the capacity differences between pre- and post-activation discharge curves.

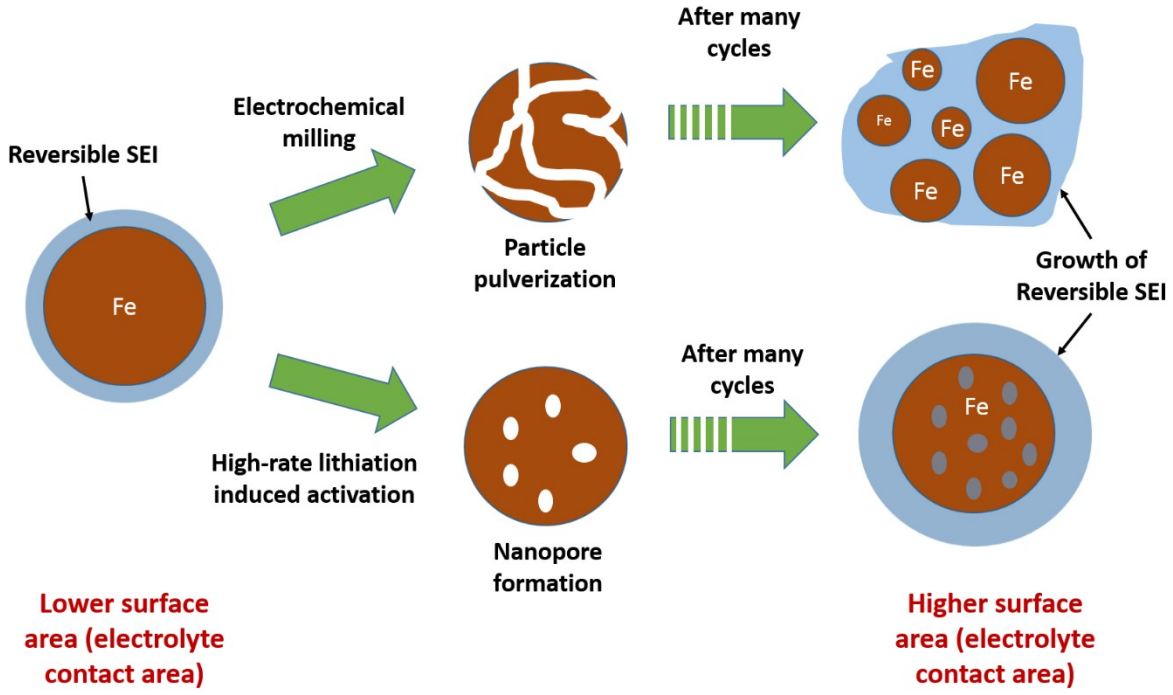

Fig. S6 Two possible activation mechanisms of iron oxide. Electrochemical milling or pulverization induced particles size reduction (top) and high-rate lithiation-induced activation (bottom). Note at low potential, iron nanoparticles (instead of iron oxide) and reversible SEI are presented.

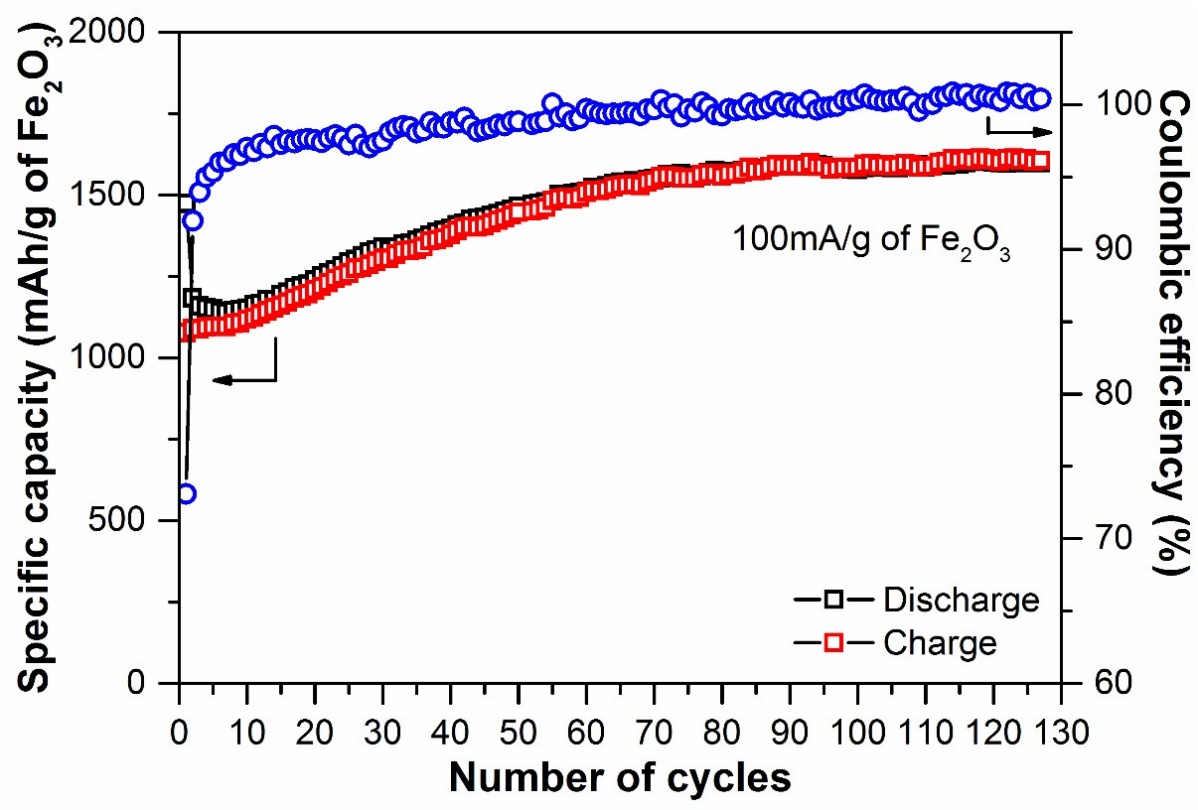

Fig. S7 Additional cycling data of γ-Fe_2O_3 NPs at 100mA g^{-1}.